Local density of states of atoms interacting with finite-bandwidth surfaces: Spin-statistics effects

Marcelo A. Romero and Edith C. Goldberg
Instituto de Desarrollo Tecnológico (CONICET-UNL) and Facultad de Ingeniería Química, UNL, cc91, 3000 Santa Fe, Argentina
(Received 11 July 2006; revised manuscript received 5 October 2006; published 15 November 2006)

The density of states on atoms interacting with solid surfaces is a required physical quantity for the understanding of processes related to scanning tunneling and photoemission spectroscopy, single-atom conductance, and emission and scattering of atoms from surfaces. In this work, we present a model calculation that allows including the localized aspects of atomic interactions and the extended features of the surface, together with alternative treatments of the Coulomb repulsion terms in the atom site. The effects of the spin fluctuation statistics treated up to a second order in the atom-surface coupling term are especially explored in this case. This approximation is comparatively analyzed with the exact results available in a model system of four levels and then used in the description of hydrogen interacting with an Al surface. Effects due to finite bandwidth and energy dependence of the local surface density of states are discussed.

DOI: 10.1103/PhysRevB.74.195419 PACS number(s): 68.43.−h, 71.10.−w, 73.23.Hk, 73.20.Hb

I. INTRODUCTION

How localized and delocalized electrons interact in atom-surface systems is a central question to many problems in condensed matter physics. The atom density of states and the change in the total density of states due to the interaction are quantities required for solving and understanding the physics in a variety of different kind of processes. For instance, scanning tunneling and photoemission spectroscopy have been extensively used to investigate the modification of surface electronic structure by magnetic and nonmagnetic adatoms, through the knowledge of the local density of states (LDOS), within a wide energy range around the Fermi level.[1–8] Also, to obtain the energy transfer rates in nearly adiabatic processes of adsorption reactions, in which hot electrons or holes are then detected as chemicurrents,[9,10] require the instantaneous LDOS.[11] The adatom LDOS is always assumed close to the ground state density in these cases.

Because of the importance of a proposal accounting for both the characteristics of surface band structure and the localized nature of atom-atom interactions, we present in this work a calculation of the density of states on atoms in front of a surface. This is done by including a detailed description of atom-surface interaction from the knowledge of the unperturbed surface density of states and the localized properties of the atoms involved. The Coulomb repulsion term in the atom site is taken into account in this case through the spin fluctuation statistics that are introduced by considering the infinite correlation limit. The atom density of states is obtained here by using a consistent motion equation method based on a slave-boson version of the Anderson Hamiltonian. The Anderson impurity model[12] is commonly used to describe the physics of magnetic impurity in a conducting host, and exhibits different types of behavior, such as mixed valence and the Kondo effect. In the case of a flat band approximation, the conduction electron bandwidth represents the largest energy scale in the problem. This is not the case of finite-bandwidth substrates in which arises the possibility of localized states. The solution obtained to a strict second order in the atom-surface hopping parameter (V^2) is able to reproduce the qualitative features of the atom density of states in the three strong correlation regimes (Kondo, mixed valence, and empty orbital), and provides occupations in an excellent agreement with exact results.[13] A solution to order V^4 improves the Kondo peak in the Kondo regime, and practically reproduces the numerically exact results in the other two regimes.[14] In the present work, we will use the V^2 solution together with an atom-surface interaction model that has been widely used in chemisorption and collision processes.[15,16] Thus, a rich variety of ingredients related to localized properties of atomic interactions and extended features of solid states are introduced in the calculation of the atom LDOS (Sec. II). In Sec. III a comparative analysis with the exact results in the four-level system case is performed, showing that the main features of the exact atom density of states are quite well captured by the second-order solution. Afterwards, we analyze the case of a hydrogen atom interacting with an aluminum surface by considering the spin-fluctuation statistics in the charge exchange. Two different situations are analyzed depending on the hydrogen charge states allowed in each one. Then, it is accounted for only neutral and positive charge states in one situation, and for only neutral and negative charge states in the other one. The density of states when only $H^0 \leftrightarrow H^+$ is involved shows a Kondo regime in which the resonance turns to be a localized state as the atom gets closer to the surface. While in the case of allowing only $H^0 \leftrightarrow H^-$, which sounds appropriate for describing the adsorption process, the three regimes are observed in the behavior of the LDOS as a function of the atom-surface distance. The comparison with the spinless approximation allows us to infer the importance of correlation effects in stationary as well as in nonequilibrium processes such as ion scattering experiments.[17,18] In these cases, it is concluded that negative hydrogen formation occurs after an efficient neutralization process on either protons or negative ions during the incoming trajectory. Our model calculation is also adequate for describing nonequilibrium stationary phenomena, such as the conductance through single atoms in the case of metallic contacts. These precisely represent cases in which neither the bandwidth is the largest energy nor is the energy dependence of the surface LDOS negligible.

 ©2006 The American Physical Society

II. THEORY

The atom-surface interacting system is described by a previously developed bond-pair model Hamiltonian that looks exactly the same as an extended version of the Anderson Hamiltonian,[15,16]

$$H = \sum_{\vec{k},\sigma} \varepsilon_{\vec{k}} \hat{n}_{\vec{k}\sigma} + \sum_{a,\sigma} \left\{ E_a^\sigma + \frac{1}{2} \sum_b \left[J_{ab} \hat{n}_{b-\sigma} + (J_{ab} - J_{ab}^x) \hat{n}_{b\sigma} \right] \right\} \hat{n}_{a\sigma} + \sum_{a,\vec{k},\sigma} \left(V_{a\vec{k}}^\sigma \hat{c}_{a\sigma}^\dagger \hat{c}_{\vec{k}\sigma} + \text{h.c.} \right).$$

In this expression, $\vec{k}$ refers to the solid states that include also the narrow core bands, and a,b to the localized atom state; E_a^σ includes the energy level of the isolated atom, crystal-field terms, and correction terms proportional to overlaps; J_{ab} and J_{ab}^x are the direct and exchange Coulomb integrals. The hopping term $V_{a\vec{k}}^\sigma$ includes also two electron interactions considered within a mean field approximation. Details of this model have been given in Ref. 15 and will be omitted here. However, it is important to remark that the Hamiltonian parameters are completely defined from the properties of the unperturbed solid given fundamentally by its density of states, and the characteristics of the involved atoms through a good set of atomic basis functions. Here it is considered only one degenerate state on the atom site with energy $E_a^\sigma = \varepsilon_a$, then

$$H = \sum_{\vec{k},\sigma} \varepsilon_{\vec{k}} \hat{n}_{\vec{k}\sigma} + \sum_\sigma \left(\varepsilon_a + \frac{1}{2} U \hat{n}_{a-\sigma} \right) \hat{n}_{a\sigma} + \sum_{\vec{k},\sigma} \left(V_{a\vec{k}}^\sigma \hat{c}_{a\sigma}^\dagger \hat{c}_{\vec{k}\sigma} + \text{h.c.} \right). \quad (1)$$

We are interested in situations where large values of the Coulomb repulsion U limit the charge exchange between atom and surface to either one electron or one hole. In these cases, the Hamiltonian based on the slave-boson approach to Eq. (1) is adequate,

$$H = \sum_{\vec{k},\sigma} \varepsilon_{\vec{k}} \hat{n}_{\vec{k}\sigma} + \sum_\sigma \varepsilon_a \hat{n}_{a\sigma} + \sum_{\vec{k},\sigma} \left(V_{a\vec{k}}^\sigma \hat{c}_{a\sigma}^\dagger \hat{b} \hat{c}_{\vec{k}\sigma} + \text{h.c.} \right). \quad (2)$$

An auxiliary boson field $\hat{b}$, $\hat{b}^\dagger$ has been introduced with the constraint relation

$$\hat{b}^\dagger \hat{b} + \sum_\sigma \hat{n}_{a\sigma} = 1.$$

The appropriate Green functions for solving nonequilibrium processes described by Eq. (2) are the following Keldysh-Green functions:[13]

$$G_{aa}^\sigma(t,t') = i\Theta(t'-t) \langle \{ \hat{c}_{a\sigma}^\dagger(t') \hat{b}(t'), \hat{b}^\dagger(t) \hat{c}_{a\sigma}(t) \} \rangle,$$

$$F_{aa}^\sigma(t,t') = i \langle [\hat{c}_{a\sigma}^\dagger(t') \hat{b}(t'), \hat{b}^\dagger(t) \hat{c}_{a\sigma}(t)] \rangle,$$

where $\{\}$ and $[\,]$ are anticommutator and commutator, respectively. For equilibrium processes, it is enough to calculate the advanced Green function from which is obtained the atom density of states,

$$\rho_{aa}^\sigma(\omega) = \frac{1}{\pi} \text{Im}\, G_{aa}^\sigma(\omega),$$

which satisfies $\int_{-\infty}^{\infty} \rho_{aa}^\sigma(\varepsilon) d\varepsilon = 1 - \langle \hat{n}_{a-\sigma} \rangle$ due to the infinite-U constraint.

The equations of motion solved up to a second order in the atom-surface coupling lead to the following expression of the advanced Green function:[13]

$$G_{aa}^\sigma(\omega) = \frac{1 - \langle \hat{n}_{a-\sigma} \rangle - I_{-\sigma}(\omega)}{\omega - \varepsilon_a - \Sigma_0^\sigma(\omega) - \Sigma_<^\sigma(\omega)}, \quad (3)$$

which for the case of an N-fold degenerate atom state is

$$G_{aa}(\omega) = \frac{1 - (N-1)[\langle \hat{n}_a \rangle + I(\omega)]}{\omega - \varepsilon_a - \Sigma_0(\omega) - (N-1)\Sigma_<(\omega)}.$$

In this last expression, $N=2$ corresponds to the present case of a spin-degenerate state, and $N=1$ to the *spinless* approximation of the atom-surface interaction.

The quantities introduced in Eq. (3) (we prefer to keep spin indexes for clarity) are

$$\Sigma_0^\sigma(\omega) = \sum_{\vec{k}} \frac{|V_{\vec{k}a}^\sigma|^2}{\omega - \varepsilon_{\vec{k}} - i\eta},$$

$$\Sigma_<^\sigma(\omega) = \sum_{\vec{k}} \frac{|V_{\vec{k}a}^{-\sigma}|^2 \langle \hat{n}_{\vec{k}-\sigma} \rangle}{\omega - \varepsilon_{\vec{k}} - i\eta},$$

and

$$I_{-\sigma}(\omega) = \sum_{\vec{k}} \frac{V_{\vec{k}a}^{-\sigma} \langle \hat{c}_{a-\sigma}^\dagger \hat{b} \hat{c}_{\vec{k}-\sigma} \rangle}{\omega - \varepsilon_{\vec{k}} - i\eta}.$$

Here, $\langle \hat{n}_{\vec{k}\sigma} \rangle$ is the solid $\vec{k}\sigma$-state occupation and the crossed term $\langle \hat{c}_{a-\sigma}^\dagger \hat{b} \hat{c}_{\vec{k}-\sigma} \rangle$ is given by

$$\langle \hat{c}_{a-\sigma}^\dagger \hat{b} \hat{c}_{\vec{k}-\sigma} \rangle = \langle \hat{n}_{\vec{k}-\sigma} \rangle V_{\vec{k}a}^{-\sigma} \text{Re}\, G_{aa}^{-\sigma}(\varepsilon_{\vec{k}}) + \frac{P}{\pi} \sum_{\vec{K}} \langle \hat{n}_{\vec{K}-\sigma} \rangle \frac{V_{\vec{k}a}^{-\sigma} \text{Im}\, G_{aa}^{-\sigma}(\varepsilon_{\vec{K}})}{\varepsilon_{\vec{K}} - \varepsilon_{\vec{k}}}, \quad (4)$$

with P indicating the principal value. By considering an expansion of the solid states in an atomic basis set $\{\psi_j(r - R_s)\}$, with j the type of state (s,p,d) and R_s giving the atom position in the solid, one obtains

$$\phi_{\vec{k}\sigma}(r) = \sum_j C_{j,R_s}^{\vec{k}\sigma} \psi_j(r - R_s). \quad (5)$$

This kind of description requires the knowledge of partial and local density of states of the solid calculated as

$$\rho_{iR_s,jR_{s'}}^\sigma(\varepsilon) = \sum_{\vec{k}} (C_{i,R_s}^{\vec{k}\sigma})^* C_{j,R_{s'}}^{\vec{k}\sigma} \delta(\varepsilon - \varepsilon_{\vec{k}}). \quad (6)$$

By using Eqs. (5) and (6), $\Sigma_0^\sigma(\omega)$, $\Sigma_<^\sigma(\omega)$, and $I_{-\sigma}(\omega)$ can be expressed in terms of the density of states of the solid and of the atom-atom hopping integrals $V_{jR_s,a}$,

$$\Sigma_0^\sigma(\omega) = \sum_{iR_s,jR_{s'}} V_{iR_s,a} V_{jR_{s'},a} \left[P \int_{-\infty}^{\infty} \frac{\rho^\sigma_{iR_s,jR_{s'}}(\varepsilon)}{\omega - \varepsilon} d\varepsilon + i\pi \rho^\sigma_{iR_s,jR_{s'}}(\omega) \right],$$

$$\Sigma_<^\sigma(\omega) = \sum_{iR_s,jR_{s'}} V_{iR_s,a} V_{jR_{s'},a} \left[P \int_{-\infty}^{\infty} \frac{\rho^\sigma_{iR_s,jR_{s'}}(\varepsilon) f_<(\varepsilon - \mu)}{\omega - \varepsilon} d\varepsilon + i\pi \rho^\sigma_{iR_s,jR_{s'}}(\omega) f_<(\omega - \mu) \right],$$

$$\mathrm{Re}\, I_{-\sigma}(\omega) = \sum_{iR_s,jR_{s'}} V_{iR_s,a} V_{jR_s,a} P \int_{-\infty}^{\infty} d\varepsilon \frac{\rho^{-\sigma}_{iR_s,jR_{s'}}(\varepsilon)}{\omega - \varepsilon} \left[f_<(\varepsilon - \mu) \mathrm{Re}\, G^{-\sigma}_{aa}(\varepsilon) + \frac{P}{\pi} \sum_{\vec{K}} \frac{f_<(\varepsilon_{\vec{K}} - \mu) \mathrm{Im}\, G^{-\sigma}_{aa}(\varepsilon_{\vec{K}})}{\varepsilon_{\vec{K}} - \varepsilon} \right]$$

$$\mathrm{Im}\, I_{-\sigma}(\omega) = \sum_{iR_s,jR_{s'}} V_{iR_s,a} V_{jR_{s'}a} \rho^{-\sigma}_{iR_s,jR_{s'}}(\omega) \left[\pi f_<(\omega - \mu) \mathrm{Re}\, G^{-\sigma}_{aa}(\omega) + P \sum_{\vec{K}} \frac{f_<(\varepsilon_{\vec{K}} - \mu) \mathrm{Im}\, G^{-\sigma}_{aa}(\varepsilon_{\vec{K}})}{\varepsilon_{\vec{K}} - \omega} \right]. \quad (7)$$

The occupation of the surface states is given by the Fermi function $f_<(\varepsilon_{\vec{K}} - \mu)$, with μ representing the chemical potential of the surface. The eventual presence of localized surface states is accounted for by the surface density of states $\rho^\sigma_{iR_s,jR_{s'}}(\varepsilon)$. In considering the contributions of inner bands $l\sigma$ with vanishing bandwidths and energies ε_l, the real parts of $\Sigma_0^\sigma(\omega)$, $\Sigma_<^\sigma(\omega)$, and $I_{-\sigma}(\omega)$ are modified accordingly to the expressions

$$\Sigma_0^\sigma(\omega) = \sum_{iR_s,jR_{s'}} V_{iR_s,a} V_{jR_{s'},a} \left[P \int_{-\infty}^{\infty} \frac{\rho^\sigma_{iR_s,jR_{s'}}(\varepsilon)}{\omega - \varepsilon} d\varepsilon + i\pi \rho^\sigma_{iR_s,jR_{s'}}(\omega) \right] + P \sum_{l,R_s} \frac{|V_{lR_s,a}|^2}{\omega - \varepsilon_l}, \quad (8)$$

$$\Sigma_<^\sigma(\omega) = \sum_{iR_s,jR_{s'}} V_{iR_s,a} V_{jR_{s'},a} \left[P \int_{-\infty}^{\infty} \frac{\rho^\sigma_{iR_s,jR_{s'}}(\varepsilon) f_<(\varepsilon - \mu)}{\omega - \varepsilon} d\varepsilon + i\pi \rho^\sigma_{iR_s,jR_{s'}}(\omega) f_<(\omega - \mu) \right] + P \sum_{l,R_s} \frac{|V_{lR_s,a}|^2 f_<(\varepsilon_l - \mu)}{\omega - \varepsilon_l}, \quad (9)$$

$$\mathrm{Re}\, I_{-\sigma}(\omega) = \sum_{iR_s,jR_{s'}} V_{iR_s,a} V_{jR_s,a} P \int_{-\infty}^{\infty} d\varepsilon \frac{\rho^{-\sigma}_{iR_s,jR_{s'}}(\varepsilon)}{\omega - \varepsilon} \left[f_<(\varepsilon - \mu) \mathrm{Re}\, G^{-\sigma}_{aa}(\varepsilon) + \frac{P}{\pi} \sum_{\vec{K}} \frac{f_<(\varepsilon_{\vec{K}} - \mu) \mathrm{Im}\, G^{-\sigma}_{aa}(\varepsilon_{\vec{K}})}{\varepsilon_{\vec{K}} - \varepsilon} \right]$$

$$+ P \sum_{l,R_s} \frac{|V_{lR_s,a}|^2}{\omega - \varepsilon_l} \left[f_<(\varepsilon_l - \mu) \mathrm{Re} G^{-\sigma}_{aa}(\varepsilon_l) + \frac{P}{\pi} \sum_{\vec{K}} \frac{f_<(\varepsilon_{\vec{K}} - \mu) \mathrm{Im}\, G^{-\sigma}_{aa}(\varepsilon_{\vec{K}})}{\varepsilon_{\vec{K}} - \varepsilon_l} \right]. \quad (10)$$

Equations (3), (7), and (10) are solved self-consistently together with the occupation of the atom state

$$\langle \hat{n}_{a\sigma} \rangle = \int_{-\infty}^{\infty} d\omega \rho^\sigma_{aa}(\omega) f_<(\omega - \mu) = \frac{1}{\pi} \int_{-\infty}^{\infty} d\omega\, \mathrm{Im}\, G^\sigma_{aa}(\omega) f_<(\omega - \mu).$$

On the other hand, the total change of the density of states due to the presence of the adatom is given by

$$\Delta\rho^\sigma(\omega) = (1/\pi) \mathrm{Im} \left[\sum_k G^\sigma_{kk}(\omega) + G^\sigma_{aa}(\omega) - \sum_k G^{\sigma(0)}_{kk}(\omega) \right],$$

where G^σ_{kk} ($G^{\sigma(0)}_{kk}$) refers to the Green's function of the conduction electrons with (without) the adatom. By using the equations of motion for $G^\sigma_{kk'}$ and G^σ_{ak}, one finds

$$\Delta\rho^\sigma(\omega) = (1/\pi) \mathrm{Im} \left[G^\sigma_{aa}(\omega) \left(1 - \frac{\partial}{\partial\omega} \sum_k \frac{|V^\sigma_{ak}|^2}{\omega - \varepsilon_k - i\eta} \right) \right]. \quad (11)$$

The atom LDOS $\rho^\sigma_{aa}(\omega)$ and the change in the density of states of the total system $\Delta\rho^\sigma(\omega)$ show a quite different behavior, since the conduction electrons react to the presence of the adsorbate. This is not the case of a flat-band, where $\rho^\sigma_{aa}(\omega) = \Delta\rho^\sigma(\omega)$ always.

By using Eqs. (5) and (6), we can write

$$\Delta\rho^\sigma(\omega) = \rho^\sigma_{aa}(\omega) + \sum_{i,R_s} \Delta\rho^\sigma_{i,R_s}(\omega). \quad (12)$$

In Eq. (12) we have introduced the quantity

$$\Delta\rho^{\sigma}_{i,R_s}(\omega) = (-1/\pi)\mathrm{Im}\left[G^{\sigma}_{aa}(\omega)\frac{\partial}{\partial\omega}\sum_{j,R_{s'}} V_{iR_s,a}V_{jR_{s'},a} \times \int_{-\infty}^{\infty} d\varepsilon \frac{\rho^{\sigma}_{iR_s,jR_{s'}}(\varepsilon)}{\omega-\varepsilon-i\eta}\right], \quad (13)$$

which allows us to discriminate per atom and state the change in the substrate density of states.

III. RESULTS AND DISCUSSION

A. Three-atom substrate

This model system consists of a chain of four atoms, one representing the adsorbate and the other three the substrate, with a total number of electrons (n) equal to 4. The three-atom substrate accounts for an incipient solid band formation and allows for an exact calculation of the density of states on the adatom site. The Hamiltonian (1) is in this case

$$H = \sum_{\sigma,k=1,2,3}\varepsilon_k\hat{n}_{k\sigma} + \sum_{\sigma}\left(\varepsilon_a + \frac{U}{2}\hat{n}_{a-\sigma}\right)\hat{n}_{a\sigma} + \sum_{\sigma,k=1,2,3}(V_{ak}\hat{c}^{\dagger}_{a\sigma}\hat{c}_{k\sigma} + \mathrm{h.c.}).$$

For the three-atom substrate with an atom-atom hopping interaction t, and a site energy equal to 0, the energies ε_k of the "band states" are $\varepsilon_1=-\sqrt{2}t$, $\varepsilon_2=0$, and $\varepsilon_3=\sqrt{2}t$. By considering the interaction only with the "surface atom" (V_0), that is, the first atom of the three-atom chain, the hopping parameters $V_{ak}=a^k_1V_0$ are calculated as

$$V_{a1} = \frac{1}{2}V_0, \quad V_{a2} = \frac{1}{\sqrt{2}}V_0, \quad V_{a3} = \frac{1}{2}V_0.$$

The exact diagonalization of this Hamiltonian, in the case of four electrons and in the infinite-U limit, is performed within a basis set of 55 Slater determinants that contemplate only positive and neutral atom configurations.

The Lehmann representation of the Green function $G^{\sigma}_{aa}(t,t')=i\Theta(t'-t)\langle\{\hat{c}^{\dagger}_{a\sigma}(t'),\hat{c}_{a\sigma}(t)\}\rangle$ is given by

$$G^{\sigma}_{aa}(\omega) = \sum_m \frac{|\alpha^{\sigma}_m|^2}{\omega+\mathrm{I}_m-i\eta} + \sum_p \frac{|\beta^{\sigma}_p|^2}{\omega-A_p-i\eta}, \quad (14)$$

with

$$\mathrm{I}_m = (E^{n-1}_m - E^n_0),$$

$$A_p = (E^{n+1}_p - E^n_0),$$

being respectively the ionization and affinity energies. The corresponding weights are

$$\alpha^{\sigma}_m = \langle\Psi^n_0|\hat{c}^{\dagger}_{a\sigma}|\Psi^{n-1}_m\rangle,$$

$$\beta^{\sigma}_p = \langle\Psi^n_0|\hat{c}_{a\sigma}|\Psi^{n+1}_p\rangle.$$

In these expressions Ψ^n_0 is the ground state of the n-electron system, and $\Psi^{n-1(n+1)}_m$ are the eigenstates of the Hamiltonian for the four-level system with $n-1$ ($n+1$) electrons. The calculation of $G^{\sigma}_{aa}(\omega)$ requires also the exact diagonalization of the Hamiltonian in the cases of three and five electrons ($n=4$). These are performed in the infinite-U limit within basis sets of 50 and 36 Slater determinants, respectively. In this form, we are able to calculate the whole spectrum of one particle excitations. The atom density of states is obtained from Eq. (14) as

$$\rho^{\sigma}_{aa}(\omega) = \frac{1}{\pi}\mathrm{Im}\,G^{\sigma}_{aa}(\omega) = \sum_{m=1-50}|\alpha^{\sigma}_m|^2\delta(\omega+\mathrm{I}_m) + \sum_{p=1-36}|\beta^{\sigma}_p|^2\delta(\omega-A_p). \quad (15)$$

The atom-state occupation (we are considering $T=0$ K) is given by

$$\langle\hat{n}_{a\sigma}\rangle = \sum_m |\alpha^{\sigma}_m|^2,$$

and the infinite-U limit constraint implies that

$$\sum_m |\alpha^{\sigma}_m|^2 + \sum_p |\beta^{\sigma}_p|^2 = 1 - \langle\hat{n}_{a-\sigma}\rangle.$$

Let us now discuss the calculation of the density of states by using the approximated expression (3) of the advanced Green function. Due to the discrete nature of the substrate, only the real parts of $\Sigma^{\sigma}_0(\omega)$, $\Sigma^{\sigma}_<(\omega)$, and $I_{-\sigma}(\omega)$ remain. Then we have

$$\rho^{\sigma}_{aa}(\omega) = \sum_i \left[1-\langle\hat{n}_{a-\sigma}\rangle - \mathrm{Re}\,I_{-\sigma}(\omega)\right]\frac{\delta(\omega-\omega_i)}{|\partial f_{\sigma}/\partial\omega|_{\omega_i}}, \quad (16)$$

with ω_i being the root of

$$f_{\sigma}(\omega) = \omega - \varepsilon_a - \mathrm{Re}\sum_0^{\sigma}(\omega) - \mathrm{Re}\sum_<^{\sigma}(\omega) \quad (17)$$

and

$$\mathrm{Re}\,\Sigma^{\sigma}_0(\omega) = V_0^2\sum_k\frac{|a^k_1|^2}{\omega-\varepsilon_k}, \quad \mathrm{Re}\,\Sigma^{\sigma}_<(\omega) = V_0^2\sum_{kocc}\frac{|a^k_1|^2}{\omega-\varepsilon_k},$$

$$\mathrm{Re}\,I_{-\sigma}(\omega) = -V_0^2\sum_{kocc}|a^k_1|^2\sum_i\frac{[1-\langle\hat{n}_{a\sigma}\rangle-\mathrm{Re}\,I_{\sigma}(\omega_i)]}{(\omega-\varepsilon_k)(\omega_i-\varepsilon_k)|\partial f_{\sigma}/\partial\omega|_{\omega_i}} + V_0^2\sum_k|a^k_1|^2\sum_{iocc}\frac{[1-\langle\hat{n}_{a\sigma}\rangle-\mathrm{Re}\,I_{\sigma}(\omega_i)]}{(\omega-\varepsilon_k)(\omega_i-\varepsilon_k)|\partial f_{\sigma}/\partial\omega|_{\omega_i}}. \quad (18)$$

For arriving at expression (18), we have used

$$\mathrm{Re}\,G^{\sigma}_{aa}(\omega') = -\frac{1}{\pi}\int_{-\infty}^{\infty}d\omega\frac{\mathrm{Im}\,G^{\sigma}_{aa}(\omega)}{\omega-\omega'} = -\sum_i\frac{[1-\langle\hat{n}_{a-\sigma}\rangle-\mathrm{Re}\,I_{-\sigma}(\omega_i)]}{(\omega_i-\omega')|\partial f_{\sigma}/\partial\omega|_{\omega_i}}.$$

From (16), the adsorbate-state occupation results

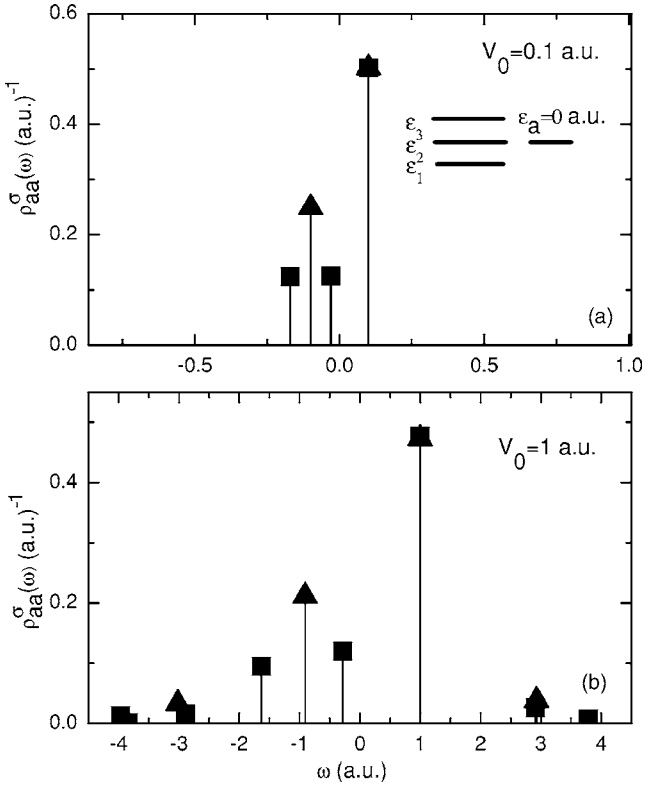

FIG. 1. Density of states on the atom site from exact (full squares) and approximated (full triangles) calculations, for atom level energy equal to 0 a.u. and for atom-surface coupling values of (a) 0.1 a.u. and (b) 1 a.u.

$$\langle \hat{n}_{a\sigma} \rangle = \sum_{iocc} \frac{[1 - \langle \hat{n}_{a-\sigma} \rangle - \mathrm{Re}\, I_{-\sigma}(\omega_i)]}{|\partial f_\sigma / \partial \omega|_{\omega_i}}. \tag{19}$$

Equations (18) and (19) are solved self-consistently by starting the calculation with initial zero values for $\langle \hat{n}_{a\sigma} \rangle$ and $I_\sigma(\omega)$.

The atom density of states given by Eq. (16) is compared with the exact one [Eq. (15)] in Figs. 1–3. Three different values of ε_a (0, −1.5, and 1.5 a.u.), and for each one, two values of V_0 (0.1 and 1 a.u.) are analyzed. In all the cases, the hopping parameter t of the three-atom chain is equal to 2 a.u. It can be observed from these figures that the approximated calculation of $\rho^\sigma_{aa}(\omega)$ resumes the main features of the exact one. The only four possible one-particle excitation energies ω_i from Eq. (17) account in an average form for the ones with relevant weights within the exact calculation (it is possible 86 one-particle excitation energies in this case). For small values of V_0 (0.1 a.u.), and the atom level energy either greater or smaller than 0 a.u., both $\rho^\sigma_{aa}(\omega)$ show practically only one $\omega_i = \varepsilon_a$. While in the case of an atom level resonant with the highest occupied substrate level ($\varepsilon_a = 0$ a.u.), this small V_0 leads to only one excitation energy below zero in the approximated calculation. This excitation energy results to be a mean value of the two exact values, with a weight equal to the sum of the corresponding exact weights. For larger values of V_0 the main differences be-

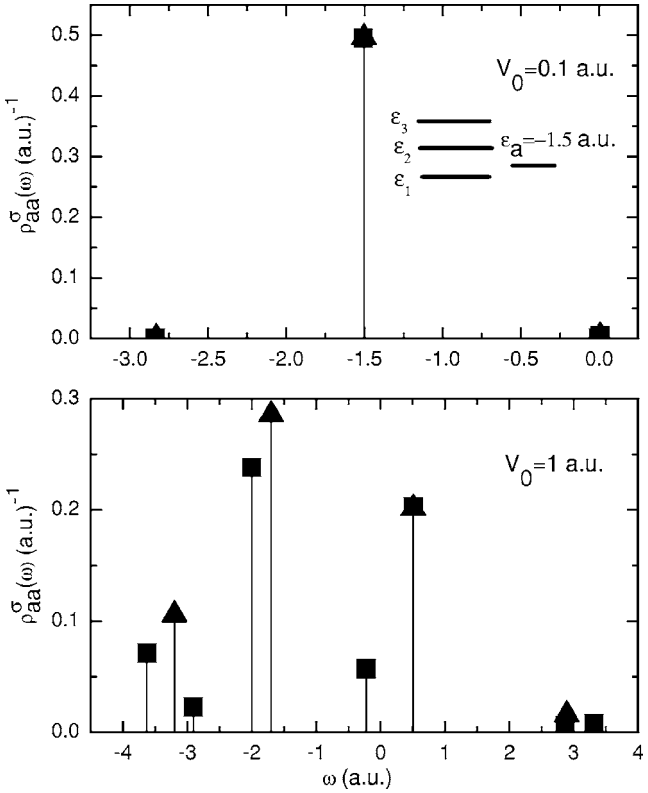

FIG. 2. The same as Fig. 1 for atom level energy equal to −1.5 a.u.

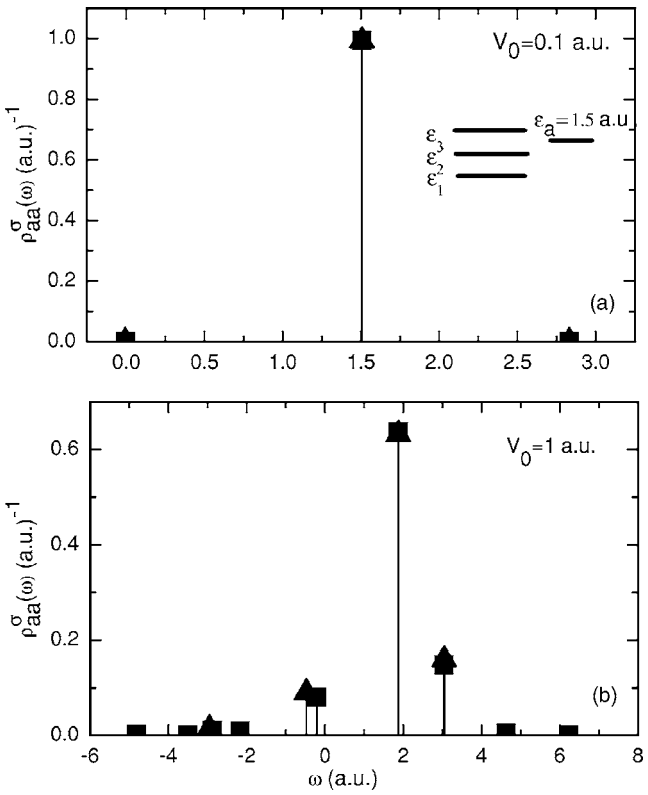

FIG. 3. The same as Fig. 1 for atom level energy equal to 1.5 a.u.

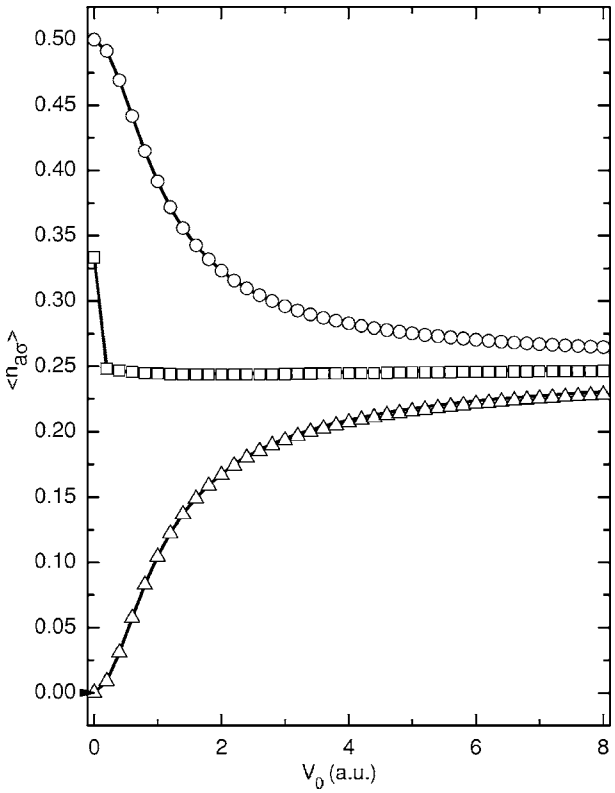

FIG. 4. Atom occupation per spin as a function of the atom-surface coupling value. Solid lines represent the exact calculation; empty symbols are the approximated results. Triangles correspond to atom energy level (ε_a) equal to 1.5 a.u., squares to ε_a=0 a.u., and circles to ε_a=−1.5 a.u.

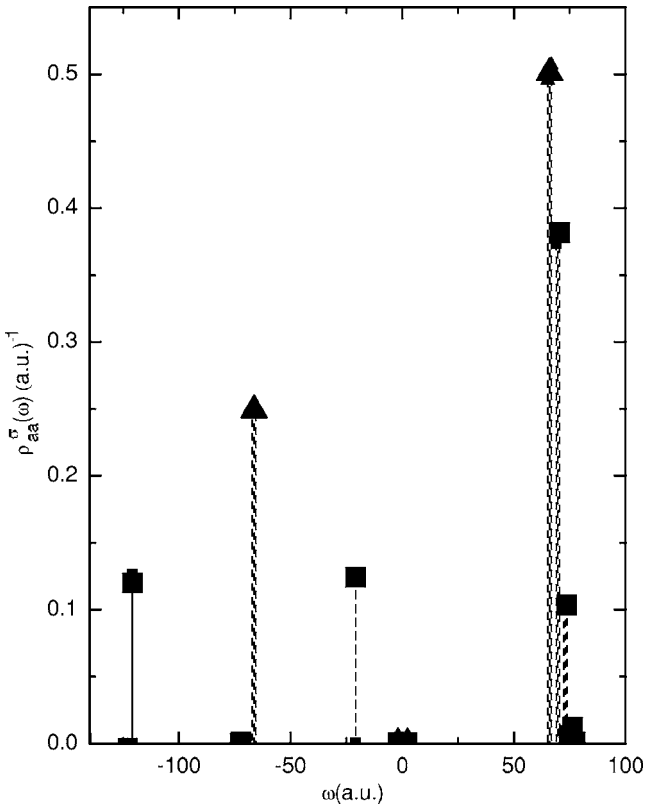

FIG. 5. Density of states on atom site for a coupling value equal to 50 a.u., and for the three values of ε_a. Full squares are the exact results and full triangles the approximated ones.

tween exact and approximated calculations occur near to the "Fermi energy" (ε_2) of the substrate in the cases that could be identified as representing Kondo (ε_a=−1.5 a.u.) and mixed valence (ε_a=0 a.u.) regimes. The empty orbital regime is the one better reproduced by the approximated calculation. But in all the cases, an excellent agreement between both calculations is observed in the hole density of states (positive excitation energies). The atom state occupations are compared in Fig. 4 for a wide range of V_0 values. The coincidence found allows concluding that the second-order approximation in the atom-substrate coupling is a very good one for calculating the atom occupations in the infinite-U limit, within either weak or strong coupling regimes.

The expression (16) accounts for the exact values in the V_0=0 limit, being in this case the expression of $\langle \hat{n}_{a\sigma} \rangle$ reduced to

$$\langle \hat{n}_{a\sigma} \rangle = \langle \hat{n}_{a-\sigma} \rangle = \int_{-\infty}^{0} [1 - \langle \hat{n}_{a-\sigma} \rangle] \delta(\omega - \varepsilon_a) d\omega.$$

We have $\langle \hat{n}_{a\sigma} \rangle$=0 for $\varepsilon_a > 0$. The values $\langle \hat{n}_{a\sigma} \rangle$=0.5 for $\varepsilon_a < 0$ and $\langle \hat{n}_{a\sigma} \rangle$=1/3 for ε_a=0, are a clear consequence of the elimination of negative atom configurations. The ground states are in these cases (considering the total spin well defined)

$$\Psi_0(\varepsilon_a = -1.5 \text{ a.u.}) = \frac{1}{\sqrt{2}} (\hat{c}^\dagger_{1\uparrow} \hat{c}^\dagger_{1\downarrow} \hat{c}^\dagger_{2\downarrow} \hat{c}^\dagger_{a\uparrow} |0\rangle \pm \hat{c}^\dagger_{1\uparrow} \hat{c}^\dagger_{1\downarrow} \hat{c}^\dagger_{2\uparrow} \hat{c}^\dagger_{a\downarrow} |0\rangle),$$

$$\Psi_0(\varepsilon_a = 0 \text{ a.u.}) = \frac{1}{\sqrt{3}} (\hat{c}^\dagger_{1\uparrow} \hat{c}^\dagger_{1\downarrow} \hat{c}^\dagger_{2\uparrow} \hat{c}^\dagger_{2\downarrow} |0\rangle + \hat{c}^\dagger_{1\uparrow} \hat{c}^\dagger_{1\downarrow} \hat{c}^\dagger_{2\downarrow} \hat{c}^\dagger_{a\uparrow} |0\rangle - \hat{c}^\dagger_{1\uparrow} \hat{c}^\dagger_{1\downarrow} \hat{c}^\dagger_{2\uparrow} \hat{c}^\dagger_{a\downarrow} |0\rangle).$$

The occupation $\langle \hat{n}_{a\sigma} \rangle$ shows an abrupt change from 1/3 to 1/4 for V_0 tending to zero in the ε_a=0 a.u. case. This change is due to the singlet nature of the ground state of the interacting system in the infinite-U limit,[19]

$$\Psi_0(\varepsilon_a = 0,\ V_0 \cong 0) = \frac{1}{\sqrt{2}} \Bigg(\hat{c}^\dagger_{1\uparrow} \hat{c}^\dagger_{1\downarrow} \hat{c}^\dagger_{2\uparrow} \hat{c}^\dagger_{2\downarrow} |0\rangle + \frac{1}{\sqrt{2}} \big[\hat{c}^\dagger_{\uparrow} \hat{c}^\dagger_{1\downarrow} \hat{c}^\dagger_{2\downarrow} \hat{c}^\dagger_{a\uparrow} |0\rangle - \hat{c}^\dagger_{1\uparrow} \hat{c}^\dagger_{1\downarrow} \hat{c}^\dagger_{2\uparrow} \hat{c}^\dagger_{a\downarrow} |0\rangle \big] \Bigg).$$

The symmetry of the interacting system for ε_a=0 fixes practically in 1/4 the atom occupation for any V_0, and the same situation is recovered for the other values of ε_a when $V_0 \gg \varepsilon_a$ and $V_0 \gg t$. The atom density of states is shown in Fig. 5 for a large V_0 value. It is observed that the three ε_a values lead practically to the same density of states. There

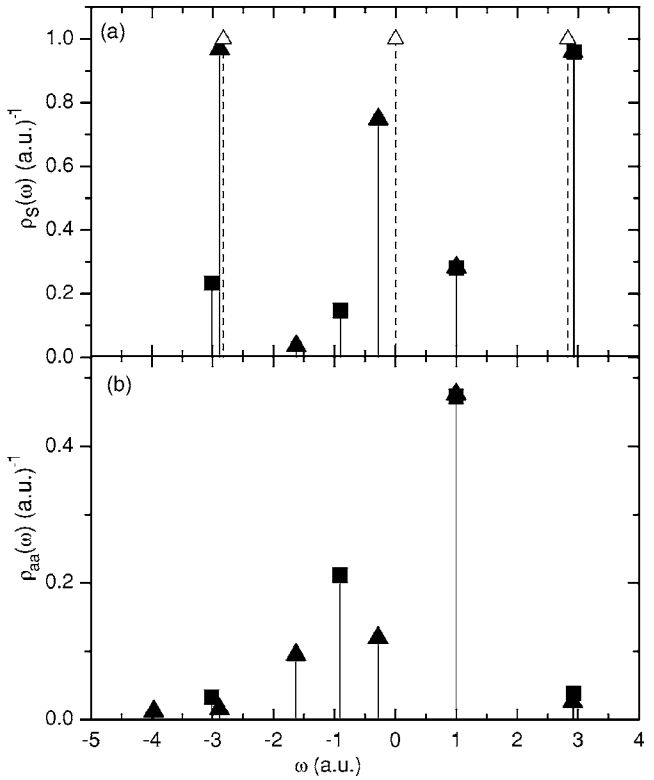

FIG. 6. (a) Density of states of the substrate $[\rho_s^\sigma(\omega)]$ in the $\varepsilon_a=0$ a.u. case. Full squares are the exact results and full triangles the approximated ones; empty triangles correspond to the unperturbed substrate density of states. (b) LDOS on atom site, full squares are the exact calculation, and full triangles the approximated one.

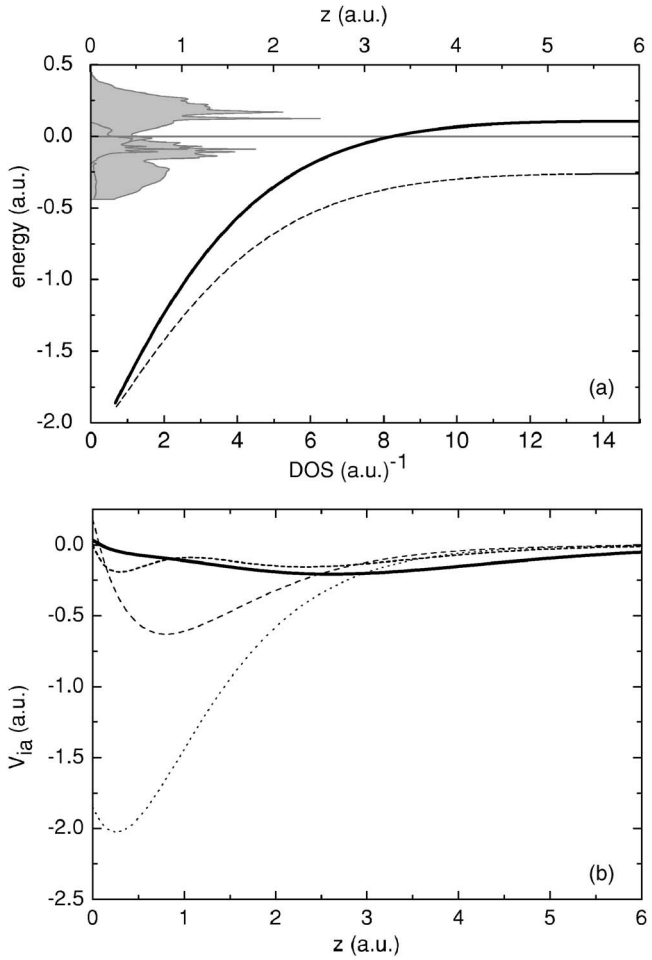

FIG. 7. (a) Ionization (dash line) and affinity (solid line) levels of hydrogen as function of distance from Al surface; the gray shadowed figure corresponds to the Al(100) LDOS. The Fermi energy is indicated by a gray line. (b) H-Al coupling parameters as function of surface distance; dotted line corresponds to the coupling with the Al-2s, long dash line to Al-2p_z, dash line to Al-3s, and solid line to Al-3p_z.

are only three excitation energies in the exact calculation case, which is characteristic of a two-degenerate level system in the infinite-U limit.[19]

In Fig. 6, the substrate density of states $\rho_s^\sigma(\omega) = \frac{1}{\pi}\,\mathrm{Im}\Sigma_k G_{kk}^\sigma(\omega)$ obtained by using either the exact calculation of $G_{aa}^\sigma(\omega)$ or the approximated expression given by Eq. (3) can be observed. The atom density of states from both calculations is also shown in this figure. These results correspond to the case $\varepsilon_a=0$, but the discussion is completely valid for the other cases too. The differences found between the exact and approximated one-particle excitation energies are more dramatic in the calculation of $\rho_s^\sigma(\omega)$ due to the factor $(\partial/\partial\omega)\Sigma_0(\omega)$ [see Eq. (11)], which depends strongly on the energy separations between ω_i and the nonperturbed substrate eigenvalues ε_k. As it can be seen from Fig. 6, the exact calculation ensures the conservation of the total number of electrons given by the identity

$$\int_{-\infty}^{0} d\omega[\rho_{aa}^\sigma(\omega) + \rho_s^\sigma(\omega) - \rho_s^{\sigma(0)}(\omega)] = 0.$$

But this relation is far from being accomplished by the approximated calculation, which gives a poor description of the $\rho_s^\sigma(\omega)$ for the negative excitation energies in this very discrete system.

B. Hydrogen interacting with aluminum surface

Here we consider an on-top adsorption configuration. The atom energy and hopping terms are obtained from an adiabatic calculation of the atom-surface interaction within a mean field approximation with atom occupations frozen at their values in the noninteracting limit. This calculation is the same one used successfully in the description of the hydrogen scattering by Al(100) surface.[18] All the one- and two-electron atomic integrals required for the calculation are provided by a quantum chemistry code,[20] by using the GAUSSIAN atomic orbitals given by Huzinaga.[21] The local and partial density of valence states $\rho_{iR_s,jR_s'}^\sigma(\varepsilon)$ for the Al(100) surface is calculated through a decimation technique,[22] and the Al-core bands are considered as localized states with energies equal to the experimental values obtained from x-ray photoemission spectroscopy data.[23]

We consider two different situations: one in which the infinite-U limit allows for only neutral and positive charge

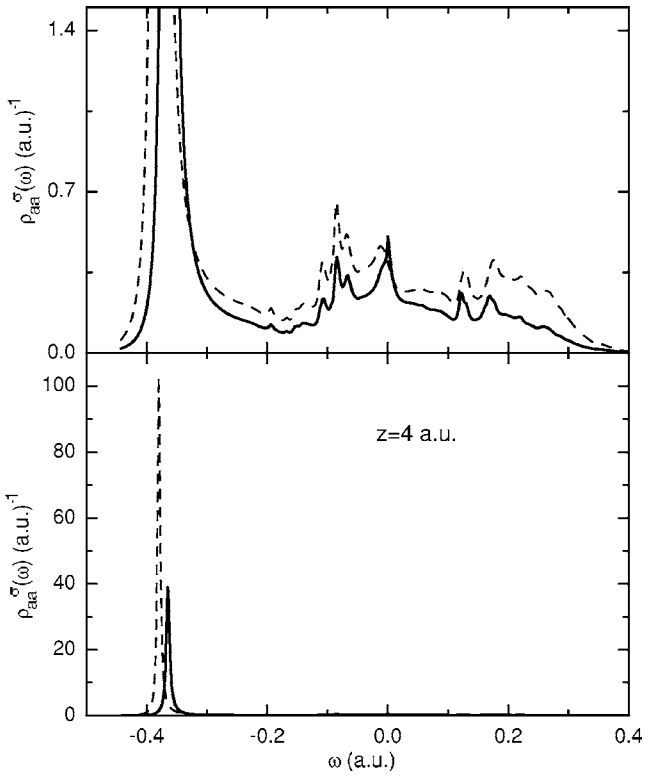

FIG. 8. Density of states on H site in the case of $H^0 \leftrightarrow H^+$, in front of Al surface for a distance value of 4 a.u. Solid line corresponds to $N=2$ and dash line to $N=1$. The top figure is a zoom of the bottom one.

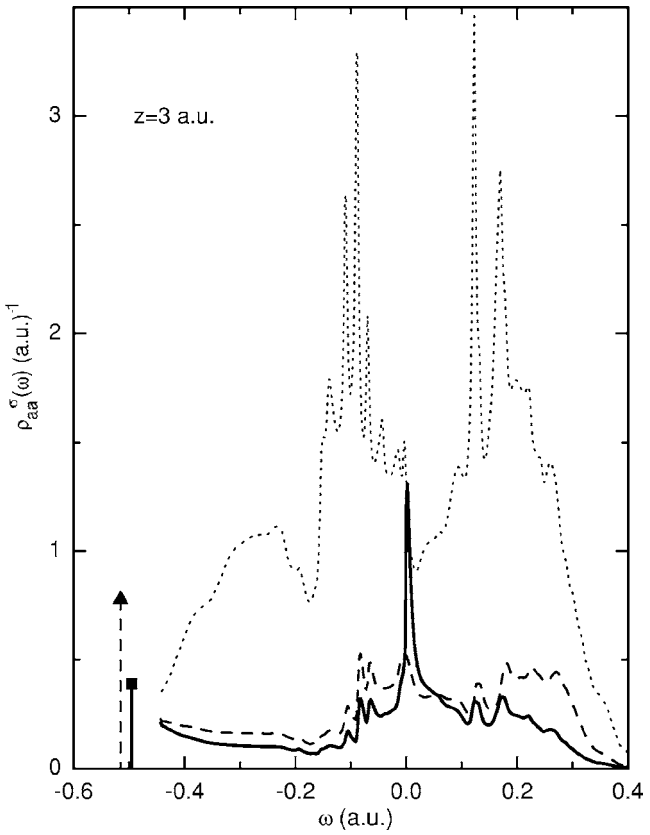

FIG. 9. The same as in Fig. 7 for a distance value of 3 a.u. Solid line and full square correspond to $N=2$, dash line and full triangle to $N=1$. It is also shown the Al(100) density of states (dotted line).

states, and the other in which the infinite-U limit allows for only neutral and negative charge states. In the slave-boson approximation, the first case has to be with two strongly correlated electrons, while the second one has to be with two strongly correlated holes.

The hydrogen level shift in front of Al surface is calculated by joining the mean field calculation that takes into account the short-range interactions, with the correct behavior by the image potential at large distances.[18] This means to consider

$$\varepsilon_a(z) = \left\{ \begin{array}{c} \tilde{\varepsilon}_a(z) - \tilde{\varepsilon}_a(z_A) + \varepsilon_\infty + V_{im}(z_A) \quad \text{for } z < z_A \\ \varepsilon_\infty + V_{im}(z) \quad \text{for } z \geq z_A, \end{array} \right\}$$

where $\tilde{\varepsilon}_a(z)$ corresponds to the calculation including the short-range interactions, and z_A (=8 a.u.) is the distance at which the join with the correct behavior by the image potential $V_{im}(z)$ is performed. The asymptotic value of the atom energy level is given by ε_∞. In the case of the ionization level $(E_0^n - E_0^{n-1})$, we have $\varepsilon_\infty = -0.5$ a.u. and $V_{im}(z) = 1/[4(z-z_0)]$. While for the affinity level $(E_0^{n+1} - E_0^n)$, $\varepsilon_\infty = -0.0276$ a.u. and $V_{im}(z) = -1/[4(z-z_0)]$. The z_0 distance corresponds to the image plane position for the Al(100) surface (3.06 a.u.). In this way, a good agreement with other existing results is obtained.[24,25]

In Fig. 7(a), the ionization $(E_0^n - E_0^{n-1})$ and affinity $(E_0^{n+1} - E_0^n)$ levels are shown as a function of the normal distance (z) to the last atomic plane of the surface. The Al(100) local density of states are also shown in this figure. The reference in energy in Fig. 7(a) is the Al Fermi level, positioned at −4.36 eV with respect to the vacuum level. In Fig. 7(b), the Al-H hopping terms $V_{jR_0,a}$, where j indicates the atomic states $2s$, $2p_z$, $3s$, and $3p_z$ of the aluminum atom situated at $R_0 = (0,0,0)$, are shown as a function of z. In all the following analysis, we consider the renormalized atom-surface coupling $V_{ak}/\sqrt{N}$ as to make possible the comparison with the $N=1$ case; and the density of states $\rho_{aa}^\sigma(\omega)$ is calculated by considering in Eqs. (7)–(10) the contribution of only the nearest aluminum atom $R_s = R_0$. The effect of Al core-bands in the atom LDOS calculation was negligible for the analyzed range of distances.

1. *Only* $H^0 \leftrightarrow H^+$ *involved*

The atom density of states $\rho_{aa}^\sigma(\omega)$ is shown in Figs. 8 and 9 for two different distances, $z=4$ and 3 a.u., respectively, and for $T=0$ K. In the first case ($z=4$ a.u.), a pronounced narrow resonance appears close to the bottom of the valence band at ω around −0.36 a.u., suggesting the formation of a localized state which becomes clearly defined in the $z=3$ a.u. case (Fig. 9). The negligible contribution of the virtual states showing a Kondo structure for $z=4$ a.u. becomes more important for $z=3$ a.u. In this case, a well-defined Kondo peak is observed at $\omega \cong 0.0018$ a.u. (0.05 eV). The other peaks located to the left and right of the Kondo peak

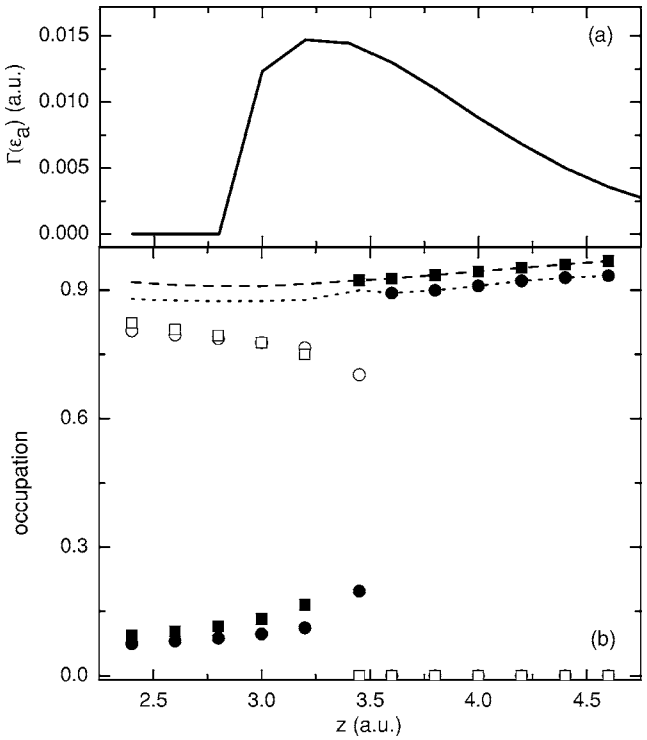

FIG. 10. (a) The level width at the ionization level energy as function of surface distance, (b) atom state occupations from $N=2$ (dash line) and from $N=1$ (dot line) calculations. Empty symbols are the contributions from localized state and full symbols are from virtual states (squares correspond to $N=2$ and circles to $N=1$ calculation).

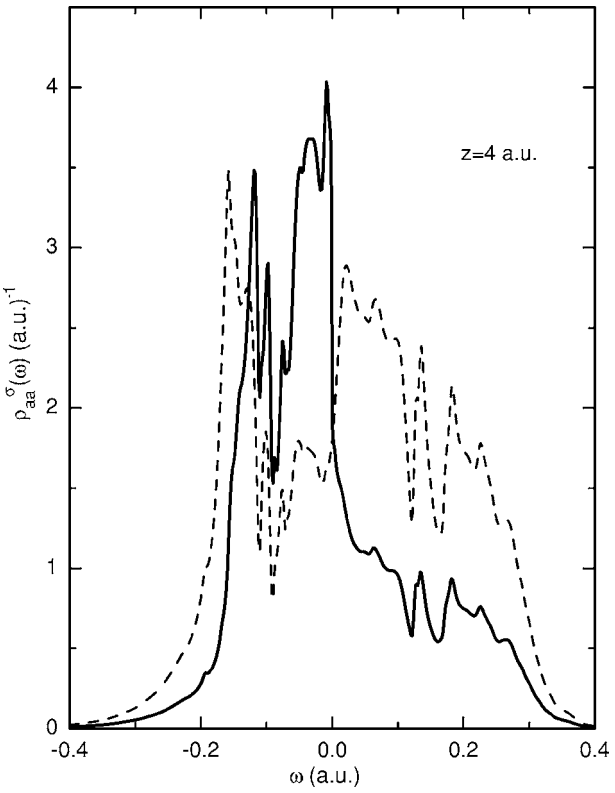

FIG. 11. Hole density of states for H^- in the case of $H^0 \leftrightarrow H^-$, in front of Al surface for a distance value of 4 a.u. Solid line corresponds to $N=2$ and dash line to $N=1$ calculation.

are originated in the Al LDOS, as it can be seen from Fig. 9. The main differences with the $N=1$ approximation occur around the Fermi level, where no pronounced peak structure is registered by the spinless calculation. The localized state (Fig. 9) arises when

$$\omega_i - \varepsilon_a - \mathrm{Re}[\Sigma_0(\omega_i) + (N-1)\Sigma_<(\omega_i)] = 0$$

and

$$\mathrm{Im}[\Sigma_0(\omega_i) + (N-1)\Sigma_<(\omega_i)] = 0.$$

According to Eq. (9) $\mathrm{Re}[\Sigma_<(\omega_i)]$ would lead to a smaller value of ω_i in the case of $N=2$ compared with $N=1$. But due to the coupling renormalization, we have in the strong correlation case

$$\mathrm{Re}[\Sigma_0(\omega_i) + \Sigma_<(\omega_i)] = \frac{1}{2}\sum_{i,j} V_{i,a}V_{j,a}P \times \int_{-\infty}^{\infty} \frac{\rho^{\sigma}_{i,j}(\varepsilon)}{\omega_i - \varepsilon}[1 + f_<(\varepsilon)]d\varepsilon,$$

while in the $N=1$ case

$$\mathrm{Re}[\Sigma_0(\omega_i)] = \sum_{i,j} V_{i,a}V_{j,a}P \int_{-\infty}^{\infty} \frac{\rho^{\sigma}_{i,j}(\varepsilon)}{\omega_i - \varepsilon}d\varepsilon.$$

In this way, the $N=2$ case leads to a larger value of ω_i.

The level width at the atom-level energy $\Gamma(\varepsilon_a)$ is calculated as

$$\Gamma(\varepsilon_a) = \mathrm{Im}[\Sigma_0(\varepsilon_a) + (N-1)\Sigma_<(\varepsilon_a)] = \frac{\pi}{N}\sum_{i,j} V_{i,a}V_{j,a}\rho^{\sigma}_{i,j}(\varepsilon_a)[1 + (N-1)f_<(\varepsilon_a)],$$

and the atom state occupation are shown in Fig. 10 as a function of surface distance z. In this case where ε_a is always below the Fermi energy, both $\Gamma(\varepsilon_a)$ from $N=2$ and $N=1$ calculations are equal. The occupations are very similar, being always larger in the $N=2$ case. When atom-surface interaction is significant, the high neutral fraction is practically determined by the contribution of the localized state ($z < 4$ a.u.). We can observe that the presence of the localized state disappears in the $N=2$ case for smaller distances than in the $N=1$ case, giving place to another important difference between them. The virtual states have the significance that their energy, translated into complex frequency, governs the time evolution of the atom state.[26] Therefore, less neutralization is expected in the case of nonequilibrium processes, due to the pronounced downshift of the atom level, the magnitude of the atom-atom coupling terms, and the energy dependence of the Al surface LDOS. The differences between $N=1$ and $N=2$ arising in the density of states around the Fermi energy are not expected to be relevant in defining the neutral fractions in ion scattering processes, while it can be important in stationary processes related with electronic transport.

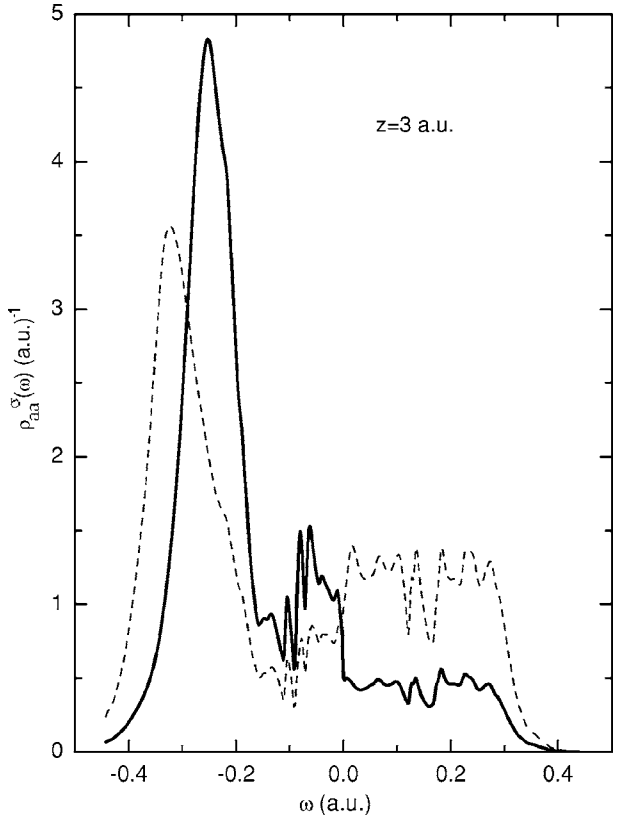

FIG. 12. The same as in Fig. 11 for a distance value of 3 a.u.

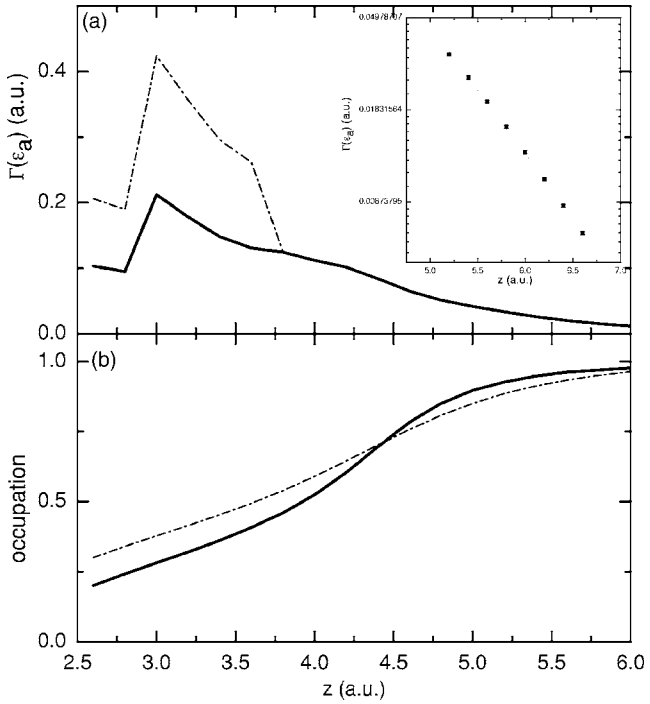

FIG. 13. (a) The level width at the affinity level energy as function of surface distance, solid line corresponds to $N=2$ and dot-dashed line to $N=1$. The inset shows the decaying exponential behavior of the level width for large distances. (b) Atom state occupations from $N=2$ (solid line) and from $N=1$ (dot-dashed line) calculations.

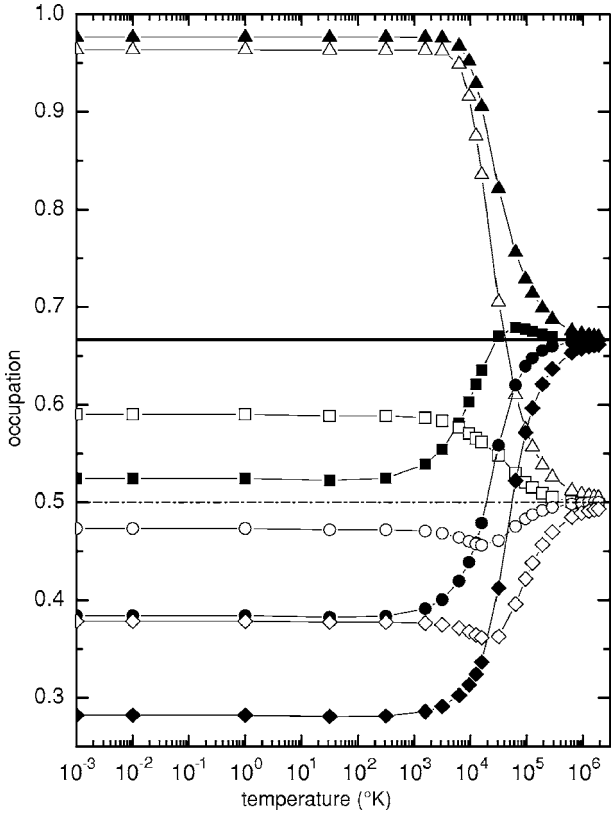

FIG. 14. Atom state occupation as function of temperature. Full symbols correspond to $N=2$ and empty symbols to $N=1$ calculation. Triangles are for surface distance equal to 6 a.u., squares to 4 a.u., circles to 3.5 a.u., and rhombus to 3 a.u. The infinite temperature limit values, 2/3 for $N=2$ and 1/2 for $N=1$, are indicated by solid and dot-dashed lines, respectively.

In this on-top configuration at $z=3$ a.u., a high Kondo temperature $T_K \sim 570$ K is obtained. Then, there is no practical variation with temperature in this case, since $T \gg T_K$ is required for it. That means that correlation effects are still present at room temperature.

2. Only $H^0 \leftrightarrow H^-$ involved

The negative charge state in the infinite-U limit is taken into account by considering two strong correlated holes; this means that the hole-state occupation $\langle \hat{n}_{a\uparrow} \rangle + \langle \hat{n}_{a\downarrow} \rangle$ provides the neutral fraction. In the hole picture,

$$f_<^{holes}(\varepsilon) = 1 - f_<^{electrons}(\varepsilon).$$

The occupied hole states correspond to $\omega > 0$; this means that

$$\langle \hat{n}_{a\sigma} \rangle = \int_{-\infty}^{\infty} \rho_{aa}^{\sigma}(\omega) f_<^{holes}(\varepsilon) d\omega,$$

$$\langle \hat{n}_{a\uparrow} \hat{n}_{a\downarrow} \rangle = \int_{-\infty}^{\infty} \rho_{aa}^{\sigma}(\omega) f_<^{electrons}(\varepsilon) d\omega = 1 - \langle \hat{n}_{a\uparrow} \rangle - \langle \hat{n}_{a\downarrow} \rangle.$$

The atom density of states $\rho_{aa}^{\sigma}(\omega)$ for distances $z=4$ and 3 a.u., and for $T=0$ K, are shown in Figs. 11 and 12, respectively. In the $z=4$ a.u. case, a LDOS characteristic of the

mixed valence regime is observed, while a transition to the empty orbital regime is taking place at smaller surface distances ($z=3$ a.u.). Pronounced differences with the uncorrelated case $N=1$ are obtained for $\omega<0$ (empty hole states). In Fig. 13, the neutral fraction or hole-state occupation is shown as a function of surface distance. The evolution of the occupation behavior from $\langle \hat{n}_a \rangle \ll 1$ to $\langle \hat{n}_a \rangle = 1$ indicates the different regimes in the $N=2$ case. The transition between the empty orbital for $z<4$ a.u. and the Kondo regime for $z>5$ a.u. occurs with a change of slope associated to the valence mixed one. This behavior, depending on the atom-level position respect to the Fermi energy, is strongly related to the spin statistics; therefore, it cannot be registered by the spinless calculation.

In Fig. 13, $\Gamma(\varepsilon_a)$ is shown as a function of surface distance. In the inset of Fig. 13(a), an exponentially decaying behavior of the level width can be observed for large distances ($z>5$ a.u.). The values obtained are in good agreement with those calculated by other methods.[27] The atom-level energy becomes resonant with the empty hole-band states for distances smaller than 3.8 a.u., in this case being $\Gamma(\varepsilon_a)_{N=2}=(1/2)\Gamma(\varepsilon_a)_{N=1}$. In this form, spin-statistical factors appear, defining the capture rate of holes equal to $\Gamma(\varepsilon_a)_{N=1}$ and the loss rate of holes equal to $(1/2)\Gamma(\varepsilon_a)_{N=1}$.[27] As a direct consequence, the main differences between occupation values from $N=2$ and $N=1$ calculations occur in the empty orbital regime. The atom-level width in $H^0 \leftrightarrow H^-$ is larger than in $H^0 \leftrightarrow H^+$. This fact is related with a larger substrate density of states at energies around the affinity level [Fig. 7(a)]. Then, the neutralization of negative ions is mainly defined by the contribution of virtual states, making it possible to infer the charge exchange in dynamical processes such as ion scattering. An increasing negative ion fraction is expected the smaller the incoming and the larger the outgoing ion kinetic energies are, and major or minor differences between $N=1$ and $N=2$ calculations will be obtained depending on the ion velocity. The effects of the infinite-U limit in the empty LDOS structure are important for processes involving holes conduction.

We also calculated $\Delta\rho^{\sigma}_{i,R_0}(\omega)$ given by Eq. (13) and found that the conservation of electron number is much better satisfied in the case of extended substrates. For a distance of 3 a.u., the atom charge equal to 0.72 is mainly provided by the s-valence states of Al [$\int_{-\infty}^{0}\Delta\rho^{\sigma}_{s,R_0}(\omega)d\omega \cong -0.7$ and $\int_{-\infty}^{0}\Delta\rho^{\sigma}_{p,R_0}(\omega)d\omega \cong -0.05$)], while in the case $z=4$ a.u., similar contributions from s and p-valence states are found [$\int_{-\infty}^{0}\Delta\rho^{\sigma}_{s,R_0}(\omega)d\omega \cong -0.27$ and $\int_{-\infty}^{0}\Delta\rho^{\sigma}_{p,R_0}(\omega)d\omega \cong -0.16$]. These results show the dependence of the resonant mechanism of charge exchange on the adatom-level position respect to the valence band states.

Figure 14 shows the dependence of the occupation with temperature for the atom at different distances from the surface, and therefore for different correlation regimes. Both calculations are compared, showing the infinite temperature limits in each case: 2/3 in the $N=2$ and 1/2 in the $N=1$ case.[28] It is only in the mixed valence regime ($z=4$ a.u.) where one can observe a more significant change for $T>300$ K.

IV. CONCLUSIONS

The model calculation presented in this work is fundamentally based on the knowledge of the interacting atom states of either localized or extended nature. The Coulomb electron interactions in the localized states can be consistently contemplated within different perturbative schemes going from Hartree-Fock to infinite value limit.[13,29] We have in this form the possibility of exploring interesting correlation effects in a lot of atom-surface systems by taking into account real features originated in the properties of the involved atoms. In summary, a calculation only based on *ab initio* calculated parameters that allows describing equilibrium and nonequilibrium stationary or dynamical processes is presented.

To account for the spin fluctuations by considering $H^0 \leftrightarrow H^-$ in the adsorption process on metal surfaces represents an improvement with respect to previous model calculations based on the Hartree-Fock approximation.[15,16] In hydrogen scattering by Al surface, the spin statistics are expected to have a more significant effect in the negative ion formation from H^0 than in H^+ neutralization.

It is concluded that the use of realistic surface LDOS can provide insights about the contribution of electron correlation and surface orbitals to photoemission spectra from simple adsorption systems, and also to ion and electron spectroscopies.

ACKNOWLEDGMENTS

We are indebted to M. C. G. Passeggi and P. G. Bolcatto for a critical reading of the manuscript. This work was supported by Grants No. 03-14724 from Agencia Nacional de Promoción Científica y Tecnológica, and No. (CAI+D) 2005-002-010 from Universidad Nacional del Litoral.

[1] J. Li, W. D. Schneider, R. Berndt, and B. Delley, Phys. Rev. Lett. **80**, 2893 (1998).
[2] H. C. Manoharan, C. P. Lutz, and D. M. Eigler, Nature (London) **403**, 512 (2000).
[3] J. Merino and O. Gunnarsson, Phys. Rev. B **69**, 115404 (2004).
[4] N. Nilius, T. M. Wallis, and W. Ho, Science **297**, 1853 (2002).
[5] K. von Bergmann, M. Bode, A. Kubetzka, M. Heide, S. Blugel, and R. Wiesendanger, Phys. Rev. Lett. **92**, 046801 (2004).
[6] Ji-Yong Park, U. D. Ham, S. J. Kahng, Y. Kuk, K. Miyake, K. Hata, and H. Shigekawa, Phys. Rev. B **62**, R16341 (2000).
[7] K. Boger, M. Weinelt, and T. Fauster, Phys. Rev. Lett. **92**, 126803 (2004).
[8] J. Rubio, M. C. Refolio, M. P. López Sancho, and J. M. López Sancho, Phys. Rev. B **38**, 3142 (1988).
[9] H. Nienhaus, B. Gergen, W. H. Weinberg, and E. W. McFarland, Surf. Sci. **514**, 172 (2002).

[10] H. Nienhaus, Surf. Sci. Rep. **45**, 3 (2002).
[11] M. S. Mizielinski, D. M. Bird, M. Persson, and S. Holloway, J. Chem. Phys. **122**, 084710 (2005).
[12] P. W. Anderson, Phys. Rev. **124**, 41 (1961).
[13] E. C. Goldberg, F. Flores, and R. C. Monreal, Phys. Rev. B **71**, 035112 (2005).
[14] R. C. Monreal and F. Flores, Phys. Rev. B **72**, 195105 (2005).
[15] P. G. Bolcatto, E. C. Goldberg, and M. C. G. Passeggi, Phys. Rev. B **58**, 5007 (1998).
[16] P. G. Bolcatto, E. C. Goldberg, and M. C. G. Passeggi, J. Phys.: Condens. Matter **12**, 8369 (2000).
[17] M. Maazouz, A. G. Borisov, V. A. Esaulov, J. P. Gauyacq, L. Guillemot, S. Lacombe, and D. Teillet-Billy, Phys. Rev. B **55**, 13869 (1997).
[18] M. C. Torralba, P. G. Bolcatto, and E. C. Goldberg, Phys. Rev. B **68**, 075406 (2003).
[19] A. C. Hewson, *The Kondo Problem to Heavy Fermions* (Cambridge University Press, Cambridge, England, 1993).
[20] This calculation was performed using the commercial program GAUSSIAN98 (GAUSSIAN 98, Gaussian, Inc., Pittsburgh, PA, 1998).
[21] S. Huzinaga, J. Chem. Phys. **42**, 1293 (1965); S. Huzinaga, J. Andzelm, M. Klobukowski, E. Radzio-Andzelm, Y. Sakai, and H. Tatewaki, in *Gaussian Basis Set for Molecular Calculations*, edited by S. Huzinaga (Elsevier, Amsterdam, 1984).
[22] F. Guinea, C. Tejedor, F. Flores, and E. Louis, Phys. Rev. B **28**, 4397 (1983).
[23] J. A. Bearden and A. F. Burr, Rev. Mod. Phys. **39**, 125 (1967).
[24] P. Nordlander and J. C. Tully, Phys. Rev. Lett. **61**, 990 (1988).
[25] A. G. Borisov, D. Teillet-Billy, and J. P. Gauyacq, Nucl. Instrum. Methods Phys. Res. B **78**, 49 (1993).
[26] D. M. Newns, Phys. Rev. **178**, 1123 (1969).
[27] A. G. Borisov, D. Teillet-Billy, and J. P. Gauyacq, Surf. Sci. **278**, 99 (1992).
[28] T. A. Costi, J. Kroha, and P. Wolfle, Phys. Rev. B **53**, 1850 (1996).
[29] E. C. Goldberg and F. Flores, Phys. Rev. B **45**, 8657 (1992).